

Published in final edited form as:

J Mol Cell Cardiol. 2013 August ; 61: 111–122. doi:10.1016/j.yjmcc.2013.03.021.

Role of late sodium current as a potential arrhythmogenic mechanism in the progression of pressure-induced heart disease

Karl Toischer, MD^{*1}, Nico Hartmann, MS^{*1}, Stefan Wagner, MD¹, Thomas H. Fischer, MD¹, Jonas Herting, MS¹, Bernhard C. Danner, MD², Can M. Sag, MD¹, Thomas J. Hund, Ph.D.³, Peter J. Mohler, Ph.D.³, Luiz Belardinelli, MD⁴, Gerd Hasenfuss, MD¹, Lars S. Maier, MD⁺¹, and Samuel Sossalla, MD⁺¹

¹Abt. Kardiologie und Pneumologie / Herzzentrum, Georg-August-Universität Göttingen, Germany

²Abt. Herzund Thoraxchirurgie, Georg-August-Universität Göttingen, Germany

³Dorothy M. Davis Heart and Lung Research Institute, Dept. of Internal Medicine, The Ohio State University Wexner Medical Center, Columbus, OH

⁴Gilead Sciences, Palo Alto, CA, USA

Abstract

Aims—To determine the characteristics of the late Na current (I_{NaL}) and its arrhythmogenic potential in the progression of pressure-induced heart disease.

Methods and Results—Transverse aortic constriction (TAC) was used to induce pressure overload in mice. After one week the hearts developed isolated hypertrophy with preserved systolic contractility. In patch-clamp experiments both, I_{NaL} and the action potential duration (APD₉₀) were unchanged.

In contrast, after five weeks animals developed heart failure with prolonged APDs and the slowed I_{NaL} decay time which could be normalized by addition of the I_{NaL} inhibitor ranolazine (Ran) or by the Ca/calmodulin-dependent protein kinase II (CaMKII) inhibitor AIP. Accordingly the APD₉₀ could be significantly abbreviated by Ran, tetrodotoxin and the CaMKII inhibitor AIP. Isoproterenol increased the number of delayed afterdepolarizations (DAD) in myocytes from failing but not sham hearts. Application of either Ran or AIP prevented the occurrence of DADs. Moreover, the incidence of triggered activity was significantly increased in TAC myocytes and was largely prevented by Ran and AIP.

© 2013 Elsevier Ltd. All rights reserved.

Corresponding author: Prof. Dr. med. Lars S. Maier, FESC, FAHA Heisenberg Professor Abt. Kardiologie und Pneumologie / Herzzentrum Deutsches Zentrum für Herz-Kreislauf-Forschung Georg-August-Universität Göttingen Robert-Koch-Str. 40 37075 Göttingen Germany lmaier@med.uni-goettingen.de Phone: +49-551-396372 Fax: +49-551-3914131 .

*authors contributed equally to this work

+authors contributed equally to this work

Conflict of interests Dr. Maier receives research grants from Gilead and is involved in clinical trials with Gilead and Menarini, companies that distribute ranolazine. Dr. Sossalla and Dr. Maier receive speaker's honoraria from Berlin-Chemie.

Publisher's Disclaimer: This is a PDF file of an unedited manuscript that has been accepted for publication. As a service to our customers we are providing this early version of the manuscript. The manuscript will undergo copyediting, typesetting, and review of the resulting proof before it is published in its final citable form. Please note that during the production process errors may be discovered which could affect the content, and all legal disclaimers that apply to the journal pertain.

Western blot analyses indicate that increased CaMKII activity and a hyperphosphorylation of the Nav1.5 at the CaMKII phosphorylation site (Ser571) paralleled our functional observations five weeks after TAC surgery.

Conclusion—In pressure overload-induced heart failure a CaMKII-dependent augmentation of I_{NaL} plays a crucial role in the AP prolongation and generation of cellular arrhythmogenic triggers, which cannot yet be found in early and still compensated hypertrophy. Inhibition of I_{NaL} and CaMKII exert potent antiarrhythmic effects and might therefore be of potential therapeutic interest.

Keywords

Heart failure; hypertrophy; arrhythmias; I_{NaL} ; CaMKII; ranolazine

Introduction

Patients with heart failure either die from pump failure or life threatening arrhythmias. Major and well accepted determinants of electrical remodelling in heart failure include prolongation of the cardiac action potential (AP) and an increased sarcoplasmic reticulum (SR) Ca-leak occurring as spontaneous SR Ca-release events [1]. Both arrhythmic triggers are known to decrease the threshold of cardiac arrhythmias. A persistent Na current, also known as late Na current (I_{NaL}), has been discussed to be a potent contributor to the progression and complications of heart failure [2-10]. Under physiologic conditions Na channels open transiently and are quickly inactivated thereby generating the peak Na current (peak I_{Na}) which is responsible for the upstroke of the cardiac AP. However, some Na channels close and reopen or remain active, carrying I_{NaL} which persists throughout the whole AP. Although the amplitude of this current is very small compared to peak I_{Na} , the long persistence and its slow inactivation kinetics make this current substantial when elevated as it has been shown in pathological conditions like heart failure, ischemic metabolites, hypoxia, or pathological redox-signaling [6, 9, 11-13].

I_{NaL} is regarded as a relevant contributor to arrhythmias and its inhibition might be of antiarrhythmic potential (for review see [8, 14]). As I_{NaL} generates Na influx and thereby an inward current throughout the AP, it is expected to contribute to the prolongation of the cardiac AP making early afterdepolarizations (EADs) more likely to occur [7, 15]. Moreover, cellular Na cycling is tightly integrated with Ca homeostasis, as Na modulates the transport direction of the Na/Ca exchanger (NCX). Cellular Na overload as well as AP-prolongation stimulate the reverse mode NCX facilitating the efflux of Na in exchange for influx of Ca [1]. The net result is an elevated diastolic Ca concentration. Additionally, the cardiac ryanodine receptor (RyR2) was shown to be “leaky” in heart failure. Spontaneous SR Ca-release events, the so called Ca-sparks, occur [1, 16] and contribute to the elevation of diastolic Ca levels. Ca, once released by spontaneously opening RyR2s, can be eliminated via the NCX, which possibly generates a depolarizing current (transient inward current, I_{Ti}) that gives rise to delayed afterdepolarizations (DADs) [7, 9, 17]. Thus, an elevation of diastolic $[Ca]_i$ and changes of the cardiac RyR2 open propensity are arrhythmogenic mechanisms in failing ventricular cardiomyocytes.

There is strong evidence that I_{NaL} is increased in animal models of heart failure as well as in human heart failure [5, 9, 11, 12, 15]. However, very little is known about the role and impact of I_{NaL} in isolated cardiac hypertrophy with preserved contractility as it commonly occurs in patients suffering from hypertensive heart disease as well as from aortic stenosis. Therefore one objective of the present study was to investigate changes in I_{NaL} in the course from pressure-induced hypertrophy with preserved contractility to heart failure.

Moreover, there is controversy regarding the quantitative contribution of an increased I_{NaL} to cause AP prolongation in heart failure, and even more so in hypertrophy. As I_{NaL} induces Na-dependent Ca-overload, the impact of I_{NaL} on DADs remains to be elucidated in a pathophysiologically relevant animal model in the absence of pharmacologic I_{NaL} inducers. Therefore, the second objective of our study was to explore the role of I_{NaL} as a contributor to AP prolongation and its consequences for generation of EADs or DADs in isolated hypertrophy with preserved contractility and in heart failure.

Furthermore, we were also interested in the underlying mechanism and possible pharmacological treatment.

Methods

An expanded Methods section is available in the Online Data Supplement.

The investigation conforms to the *Guide for the Care and Use of Laboratory Animals* (NIH publication No. 85–23, revised 1996) and was approved by a local ethics review board and by the Veterinary Institute of the Lower Saxony State Office for Consumer Protection and Food Safety (G10/220).

2.1. Transverse aortic constriction (TAC) and echocardiography

8 weeks old female C57/BL6J mice were anesthetized using intraperitoneal injections of ketamine and xylazine (100 mg/kg + 5 mg/kg) and pressure overload was induced by transversal aortic constriction (27G needle). For analgesia (metamizole 1.33 mg/ml) was added to the drinking water 2 days before surgery and continued for 7 days after operation.

Transthoracic echocardiography was performed blinded using a Vevo2100 (VisualSonics, Toronto, Canada) system with a 30 MHz center frequency transducer. The animals were anesthetized with 3% isoflurane, and temperature-, respiration-, and ECG-controlled anesthesia was maintained with 1.5% isoflurane. Maximal left ventricular length (L), thicknesses of the septum, the posterior myocardial wall, the inner diameter of the left ventricle (LVEDD) and the area of the left ventricular cavity (Area) were measured according to standard procedures. The ejection fraction (EF) was calculated using the area-length method.

After completion of the experiments mice were killed in isofluran anaesthesia (5%) by cervical dislocation.

2.2. Cell isolation

The excised hearts were mounted on a Langendorff perfusion apparatus and were retrogradely perfused. Cardiomyocytes were isolated with liberase 1 (Roche diagnostics, Mannheim, Germany) and trypsin 0.6% digestion and were plated onto superfusion chambers. The glass inlays had been pretreated with laminin to allow cell adhesion and were then used for immediate measurements.

2.3. Patch-clamp experiments

Ruptured-patch whole-cell voltage- and current-clamp was used to measure action potentials and I_{NaL} as described previously [18, 19]. Measurements were performed at increasing stimulation frequencies to elicit Na currents or action potentials (APs). For Na current measurements myocytes were held at -120 mV and I_{NaL} was elicited using 250 ms depolarizing pulses to -20 mV. Each pulse was preceded by a 5 ms pre-pulse to $+50$ mV in order to optimize voltage control. The measured currents were normalized to the membrane

capacitance. I_{Na} decay (first 200 ms) was fitted using a double exponential function $y(t) = A_1 \exp(-t/\tau_1) + A_2 \exp(-t/\tau_2) + y_0$ as it was done previously [5, 18, 19].

For action potential recordings, low-resistance pipettes were used. Resting cell membrane potentials were similar in WT (-65 ± 0.94 mV), TAC (compensated hypertrophy) (-64.86 ± 0.63 mV) and in TAC (heart failure) (-64.94 ± 0.77 mV) ventricular myocytes. All patch-clamp experiments were conducted at room temperature.

2.4. Confocal microscopy

Cardiomyocytes were incubated with a Fluo-3 AM loading buffer. Experimental solution contained (mmol/L): NaCl 136, KCl 4, NaH_2PO_4 0.33, NaHCO_3 4, CaCl_2 2, MgCl_2 1.6, HEPES 10, glucose 10 (pH 7.4, NaOH, room temperature) as well as 10^{-8} mol/L isoproterenol and the respective drugs. Cardiomyocytes were continuously superfused during experiments after washing out the loading buffer and any extracellular dye. Ca-spark measurements were performed with a laser scanning confocal microscope (LSM 5 Pascal, Zeiss, Jena, Germany) using a 40x oil-immersion objective. Fluo-3 was excited by an argon ion laser (488 nm) and emitted fluorescence was collected through a 505 nm long-pass emission filter. Fluorescence images were recorded in the line-scan mode with 512 pixels per line (width of each scanline: 38.4 μm) and a pixel time of 0.64 μs . One image consists of 10,000 unidirectional line scans, equating to a measurement period of 7.68 s. Experiments were conducted at resting conditions after loading the SR with Ca by repetitive field stimulation at 4 Hz. Ca-sparks were analyzed with the program SparkMaster for Image. The mean spark frequency of the respective cell (CaSpF) resulted from the number of sparks normalized to cell width and scan rate ($100 \mu\text{m}^{-1} \cdot \text{s}^{-1}$). Spark size (CaSpS) was calculated as product of spark amplitude (F/F_0), duration and width. From this, we inferred the average leak per cell by multiplication of CaSpS with CaSpF.

2.5. Drugs

10 $\mu\text{mol/L}$ Ran ([+]*N*-(2,6-dimethylphenyl)-4-[2-hydroxy-3-(2-methoxyphenoxy)-propyl]-1-piperazine acetamide dihydrochloride) was used because it is within the range of therapeutic plasma levels and inhibitory concentrations of 50% for inhibition of I_{NaL} (6 to 15 $\mu\text{mol/L}$), which does not significantly inhibit I_{Ca} , $I_{Na/Ca}$, or I_{Ks} [10]. Tetrodotoxin (TTX) selectively blocks I_{Na} and at low concentrations relatively selective for I_{NaL} [15]. Thus, we used TTX concentrations of 2 $\mu\text{mol/L}$. Autocamide-2-related Inhibitory Peptide (AIP, 1 $\mu\text{mol/L}$) was used to selectively inhibit Ca/calmodulin-dependent protein kinase II (CaMKII). Isoproterenol was used at a concentration of 10^{-8} mol/L.

2.6. Western blots

Myocardium was homogenized and protein concentration was determined by BCA assay (Pierce Biotechnology, Rockford, USA). Denatured tissue homogenates (on ice in 2% beta-mercaptoethanol) were subjected to Western blotting (5%, 8% or 12.5% SDS-polyacrylamide gels). The antibodies used are shown in the online supplement. Chemiluminescent detection was done with Immobilon Western Chemiluminescent HRP Substrate (Millipore, Billerica, USA).

2.7. Data analysis and statistics

All data are presented as mean \pm S.E.M. Student's t-test, 2-way or 1-way repeated measures ANOVA (RM-ANOVA) with post-hoc tests were used to test for significance. A two-sided P value of <0.05 was considered significant. Blinded procedures were performed in case of echocardiographic measurements due to the variability of this technique. All other experiments were performed in an unblinded manner.

Results

3.1 Mouse cardiac phenotype

One week after TAC concentric hypertrophy was detectable, indicated by increases of septum width by 14% (sham, n=6, 0.76 ± 0.04 mm vs. TAC, n=10, 0.87 ± 0.05 mm; $p < 0.001$, Figure 1B) and heart weight by 18% (HW/BW: sham 8.0 ± 0.3 vs. TAC 9.4 ± 0.4 ; $p < 0.001$; Figure 1C). At this time point contractile function was still preserved (ejection fraction, EF: sham $49 \pm 3\%$ vs. TAC $53 \pm 7\%$; $p < 0.16$; Figure 1E).

Five weeks after TAC surgery cardiac mass was further increased by 87% (HW/BW ratio: sham 7.8 ± 0.9 vs. TAC 14.6 ± 3.1 ; $p < 0.001$; Figure 1C) and the animals showed signs of heart failure. Left ventricular EF was reduced to $33 \pm 7\%$ in TAC compared to $53 \pm 6\%$ in sham animals ($p < 0.001$; Figure 1E). Dilatation as measured by an increased LVEDD by 12% was observed in TAC compared to sham hearts (4.1 ± 0.3 mm vs. 3.6 ± 0.2 mm $p < 0.001$; Figure 1D).

Kaplan-Meier analysis of animal survival showed an increased mortality within the first days after surgery. This is followed by a stable phase with no further deaths until heart failure develops between weeks three-five after TAC intervention (Figure 1G). In this range animals were at higher risk to die and thus we investigated the role of the I_{NaL} at two time points, which are one and five weeks after surgery.

3.2 I_{NaL} in compensated hypertrophy and heart failure

One week after TAC intervention cardiomyocytes did not show significant changes of I_{NaL} compared to sham myocytes (Figure 2A). At 2 Hz I_{NaL} decay in TAC myocytes was 41.6 ± 6.5 vs. 26.7 ± 1.8 ms (at 3 Hz: 26.7 ± 4.5 vs. 26.8 ± 4.2 ms) in cells from hearts of animals that underwent sham surgery (n=17 vs. 11, $p = n.s.$, Figure 2B). Moreover, Ran had no significant effect on the small I_{NaL} of either groups (n=5 and 6, $p = 0.2$). In contrast, at five weeks after TAC surgery, I_{NaL} was significantly increased as indicated by a slower decay time (Figure 3A). At 2 Hz I_{NaL} decay time was slowed to 96.4 ± 12.6 ms compared to 35.4 ± 4.1 ms in sham myocytes ($p < 0.05$, n=26 vs. 7, Figure 3B). Superfusion with Ran, TTX as well as AIP significantly reversed the TAC-induced effect on I_{NaL} decay time (51.8 ± 5.3 ms (n=17), 47.1 ± 6.3 ms (n=15) and 29.3 ± 2.7 ms (n=18), $p < 0.05$ vs. TAC). Again, Ran had no significant influence on the small I_{NaL} recorded at five weeks in sham myocytes compared to controls (sham+Ran 35.4 ± 5.0 ms vs. control 35.4 ± 4.1 ms, n=8 vs. 7).

3.3 Role of I_{NaL} on action potential duration

To determine the arrhythmogenic role of an increased I_{NaL} we measured APs in the groups stated above. In accordance to the I_{NaL} results we did not find significant prolongations of APs in myocytes isolated from animals one week after TAC surgery (Figure 4 A and B). However, five weeks post TAC surgery the AP prolongation became noticeable. This is illustrated in figure 5A where a representative original recording shows a markedly prolonged AP in a cell isolated from a TAC animal. APD_{90} at 2 Hz was increased to 140.0 ± 24.9 ms compared to 63.1 ± 9.1 ms in myocytes isolated from sham animals (n=15 vs. 8, RM-ANOVA $p < 0.05$, Figure 5B). In these TAC myocytes with prolonged APD, Ran caused a significant abbreviation of APD_{90} to 80.0 ± 12.5 ms (n=19) while it did not shorten APD of sham myocytes (n=8). Moreover, to confirm that these effects were really due to I_{NaL} inhibition we also performed experiments in the presence of TTX. As shown in figure 5B the APD_{90} could also be reduced to 49.0 ± 9.8 ms in the presence of $2 \mu\text{mol/L}$ TTX compared to TAC control (RM-ANOVA $p < 0.05$, n=10) and was not statistical different compared to that of Ran-treated cells (Figure 5B). Moreover, using AIP as a CaMKII-

inhibitor APDs could be abbreviated to 63.4 ± 9.3 ms in cardiomyocytes that were isolated from animals five weeks after TAC surgery ($n=18$, $p<0.05$).

3.4 Potential Arrhythmogenic triggers in pressure overload-induced heart failure

To further investigate the contribution of I_{NaL} on cellular arrhythmias we exposed cardiomyocytes isolated from animals five weeks after TAC surgery to 10^{-8} mol/L isoproterenol for 5 minutes. Interestingly, we did not observe clear EADs in the presence of isoproterenol. However, there was a large number of DADs (Figure 6A) with an incidence of 2.0 ± 0.1 /min in TAC compared to 0.3 ± 0.1 DADs/min in sham cells ($n=20$ vs. 15, $p<0.05$, Figure 6B). This is important in so far that in our model DADs seem to be the major cellular arrhythmic triggers. In the presence of either Ran or AIP the incidence of DADs largely decreased to values of 0.2 ± 0.1 /min and 0.12 ± 0.1 ($n=15$ and 8, $p<0.05$, Figure 6A and B). Moreover, triggered activity never occurred in sham myocytes but was present in TAC cells with an incidence of 0.064 ± 0.025 /min ($n=15$ vs. 20, $p<0.05$ vs. sham, Figure 6C and D). When adding Ran to the bath solution triggered activity was suppressed to 0.003 ± 0.003 /min ($p<0.05$, $n=16$). Triggered activity did not occur in the presence of AIP in TAC myocytes ($n=5$, $p<0.05$ vs. TAC).

To further elucidate the underlying mechanism of DADs and triggered activity we performed measurements of spontaneous SR Ca-release events, the so called SR Ca-sparks. Figure 6F shows that the high SR Ca-spark frequency of cardiomyocytes isolated from animals five weeks after TAC surgery could be significantly suppressed from 2.1 ± 0.4 to 1.1 ± 0.3 $s^{-1} * 100 \mu m^{-1}$ upon Ran- and to 0.7 ± 0.2 $s^{-1} * 100 \mu m^{-1}$ upon AIP-treatment ($n=31$ vs. 38 vs. 30, $p<0.05$). Accordingly, the calculated SR Ca-leak was largely decreased by either inhibition of I_{NaL} or CaMKII, which was mainly driven by a reduced SR Ca-spark frequency in the presence of the respective inhibitor (Figure 6H).

3.5 Changes in Na channel expression and regulation

It has been reported that I_{NaL} is modulated by the expression of different α - and β -Na channel subunits and by phosphorylation of the $\alpha 1.5$ -isoform by CaMKII δ [2, 8, 20], [21, 22].

At the stage of compensated hypertrophy (one week after TAC surgery) the expression of the neuronal Na channel Nav1.1 was slightly downregulated by 23% ($p<0.05$) while Nav1.6 was not significantly changed. The expression of the cardiac Na channel Nav1.5 was increased dramatically by 192% ($p<0.05$) and the beta1-subunit was upregulated by 60% ($p<0.05$). CaMKII δ activity which was measured by phosphorylation at Thr-286 was increased by 45% one week after TAC surgery ($p<0.05$) while Nav1.5 phosphorylation at Ser571 was not significantly altered (Figure 7A-G).

The Nav1.1 was upregulated by 71% ($p<0.05$), whereas Nav1.6 was reduced by 29% ($p<0.05$) five weeks after TAC intervention. The Nav1.5, again, was upregulated by 57% ($p<0.05$) and the beta1-subunit showed an increase of 65% ($p<0.05$). Most importantly, the CaMKII δ activity was elevated by 108% ($p<0.05$) and the phosphorylation of Nav1.5 at Ser571 was increased by 85% ($p<0.05$, Figure 7A-G) Comparing compensated hypertrophy (one week) and heart failure (five weeks after TAC surgery) the following differences were noted. 1) The Nav1.5 is even more upregulated one week after TAC compared to five weeks after TAC intervention (-70% , $p<0.01$); 2) The Nav1.1 expression changes from downregulated to upregulated (TAC 1 vs. 5 weeks: $+185\%$, $p<0.05$); 3) CaMKII δ activity shows a further increase (TAC 1 vs. 5 weeks, $+40\%$, $p<0.05$) and 4) The Nav1.5 becomes hyperphosphorylated at the CaMKII-phosphorylation site Ser571 in hearts after five weeks but not after one week of TAC.

Discussion

The results of the present study show that 1) pressure overload-induced hypertrophy with preserved ejection fraction is neither associated with an increased I_{NaL} nor a significant prolongation of the APD. 2) In pressure overload-induced heart failure I_{NaL} is increased as indicated by a slowed decay time; 3) This increase in I_{NaL} contributes significantly to the prolonged APD as demonstrated by the effects of I_{NaL} inhibitors. 4) Failing cells developed DADs and triggered activity, which were likely caused by an increased SR Ca-leak under beta adrenergic stress. Cellular arrhythmogenic triggers could be largely prevented by either inhibition of I_{NaL} or CaMKII. 5) Slowed I_{NaL} decay time, APD prolongation and cellular arrhythmogenic triggers occurred in a CaMKII-dependent manner. 6) Western blot analyses showed an increased activity of CaMKII with a consecutive hyperphosphorylation of the Nav1.5 at Ser571 and an upregulation of the neuronal Na channel Nav1.1 in hearts after 5 weeks of TAC.

4.1 Animal model of hypertrophy and heart failure

Most of the work on I_{NaL} in combination with Ran as an inhibitor of this current has been done in models of myocardial ischemia or with pharmacological enhancers of I_{NaL} (e.g. ATX-II). We now provide data in a non-ischemic pressure overload-induced mouse model. One week after TAC surgery mice showed compensated hypertrophy with preserved systolic function and no increase in mortality, which indirectly indicates the absence of lethal arrhythmias.

Mortality increases with time during pressure overload conditions. This observation might be explained by the development of heart failure because EF markedly decreases five weeks after TAC intervention. The reason for the deaths might, however, also be lethal arrhythmias. To the best of our knowledge, telemetric recordings during the development of pressure overload-induced heart failure in mouse models have not been published so far. However, in-vivo electrophysiological measurements showed an increased rate of ventricular arrhythmias [23].

4.2 I_{NaL} and action potential duration in hypertrophy

Little is known about the I_{NaL} in pressure-induced hypertrophy, particularly in animals with preserved contractility. In hypertrophy and in the absence of heart failure (1 week of TAC) we did not find a significant increase of I_{NaL} . Likewise, these cells did not show prolonged APD, which is consistent with an unchanged I_{NaL} . Moreover, these animals had no increased risk to die suggesting that unchanged I_{NaL} and normal APD are associated with a smaller risk of sudden death. However, there are also reports of prolonged APs in pressure overload-induced heart disease [24]. Many studies did not differentiate between hypertrophy and heart failure which makes it difficult to interpret and to compare the results of these studies to the present report. Moreover, the severity of hypertrophy depends on the technique and the used protocol (e.g. needle size and time after TAC surgery). Thus, a direct comparison of results of different TAC studies is not straightforward. For example we also found a prolongation of the APD seven days after TAC operation in our previous work [24]. This difference might be explained by use of a different mouse line (FVBN previously vs. C57/BL6 here) and different age of investigated mice (12 vs. 8 weeks). The difference is also visible in the degree of hypertrophy (septum width: +18% previously vs. 14% here). This suggests that in this model the prolongation of the APD and the increased I_{NaL} are not present in compensated hypertrophy but might be one of the early changes during the development of higher degrees of hypertrophy and heart failure. In our previous work we did not investigate cardiomyocytes isolated from TAC-mice with heart failure. Moreover, I_{NaL} and its implication for APD prolongation and for cellular arrhythmogenic triggers were

evaluated in the course of the current study. Finally, the findings of a crosstalk between I_{NaL} and CaMKII in our model of afterload-induced cardiac disease have not been described before.

4.3 Role of I_{NaL} in AP prolongation in heart failure

One abnormality most consistently reported in heart failure is the prolongation of the cardiac AP. This prolongation of AP may be caused by increases in depolarizing currents such as L-type Ca or NCX current as well as due to changes in Na transport proteins (e.g. Na channels, Na/K-ATPase and Na/H-exchanger). In addition, AP prolongation in heart failure is associated with a decrease in repolarizing K currents. However, the nature of the underlying ionic currents that are responsible for APD prolongation in heart failure remains a matter of debate. In fact, an increase in I_{NaL} of ventricular myocytes of failing hearts (including humans) has been reported [2, 4, 5, 9, 12, 15].

We now provide further evidence that I_{NaL} may prominently contribute to AP prolongation in pressure-induced heart failure. Our results clearly show that I_{NaL} decay slows in parallel to AP prolongation five weeks after TAC surgery. We further demonstrate the I_{NaL} -dependence of AP prolongation by performing experiments using inhibitors of I_{NaL} . Ran is known to preferentially inhibit the late component of I_{Na} vs. peak I_{Na} but is also known to inhibit I_{Kr} with an IC_{50} of $\sim 11.5 \mu\text{mol/L}$ [25]. Thus to ascertain the role of I_{NaL} we performed experiments using TTX, as TTX specifically blocks Na channels with negligible effects on other ion current and transport systems. Both agents significantly reversed the slowed I_{NaL} decay time in parallel with a prominent abbreviation of the cardiac AP in myocytes isolated from animals five weeks after TAC surgery. Thus, it can be suggested that I_{NaL} is a major contributor to AP prolongation in pressure overload-induced heart failure.

Similar results were found by Maltsev and coworkers in myocytes isolated from human failing hearts [9]. In their experiments APD could be abbreviated up to $\sim 75\%$ by applying TTX to failing myocytes. Also two specific Na channel blockers (saxitonin and lidocaine) reduce APD in isolated cardiomyocytes from an ischemic dog heart failure model [26]. Similar results were reported by Undrovinas et al. using Ran in cells isolated from an ischemic heart failure model [27]. Moreover, a recent study also indicates that AP prolongation of myocytes from pressure overload-induced failing rat hearts could be attenuated by TTX [28]. Finally, several studies have consistently shown that pharmacological augmentation of I_{NaL} e.g. using ATX-II or ROS results in marked prolongation of the cardiac AP [6, 7, 29, 30], which could be blunted by application of Ran or TTX. Therefore, there is strong and growing evidence that elevation of I_{NaL} plays a major role in the prolongation of cardiac AP in the progression of pressure-induced heart failure.

The underlying mechanisms of I_{NaL} induction in the failing cardiomyocyte are still unclear. We now provide evidence that the prominent I_{NaL} in our mouse model of afterload-induced heart failure is CaMKII-dependent. The CaMKII inhibitor AIP significantly reversed the slowed I_{NaL} decay time and abbreviated APDs in cardiomyocytes isolated from animals five weeks after TAC surgery. Previous studies showed an elevated I_{NaL} in transgenic CaMKII δ mice, adenoviral CaMKII transfected rabbit cardiomyocytes, and guinea-pig ventricular myocytes in either the absence or presence of CaMKII that could be reversed by application of CaMKII inhibitors [2, 31]. Moreover, a recent study suggest that an increased I_{NaL} leads to activation of CaMKII, which in turn phosphorylates Nav1.5, further promoting I_{NaL} in genetically or pharmacologically modified mice cardiomyocytes [32]. Pharmacological inhibition of either CaMKII or I_{NaL} could ameliorate cardiac dysfunction caused by excessive Na influx. Thus, the present study confirms this finding and expands the knowledge in a clinically relevant model of afterload-induced heart failure.

4.4 I_{NaL} generates cellular arrhythmic triggers

Because afterdepolarizations were rarely seen under basal conditions we increased cellular SR Ca stores using isoproterenol to unmask cellular arrhythmias. Experiments under these conditions may be of clinical relevance because the isoproterenol concentrations (eg, 10^{-8} mol/L) used in our study are equivalent to catecholamine levels found in human heart failure [33]. Here we show that isoproterenol prominently induced DADs without evidence for clear induced EADs although AP prolongation was present in these TAC cells. Nevertheless, occurrence of DADs was potent enough to cause typical triggered activity as indicated by repetitive unstimulated APs.

An enhanced I_{NaL} has been reported to increase $[Na]_i$ [18] as it occurs in heart failure [34]. The increased $[Na]_i$ leads to a subsequent Ca-overload due to the extrusion of Na via the reverse mode NCX and to a decreased Ca extrusion through NCX during its operation in the forward mode [3, 18]. This increase of diastolic Ca has been shown to produce spontaneous SR Ca-release events also known as Ca-sparks [1, 3]. Ca-sparks and waves are facilitated by leaky RyR2 in heart failure [16]. Ca-sparks are believed to participate as crucial events in the initiation and propagation of Ca-waves and the elimination of cytosolic Ca via the NCX generates a depolarizing current (transient inward current, I_{TI}), which can give rise to DADs and which presumably underlies our observations [7, 9, 17].

Ran had strong antiarrhythmic effects by reducing the incidence of DADs and triggered activity in TAC myocytes most likely by attenuating the Na-induced Ca-overload resulting in a lower incidence of spontaneous SR Ca-release events as it was shown previously in failing cardiomyocytes [3, 7, 35]. Preliminary data from our group indicate that augmentation of I_{NaL} activates CaMKII which phosphorylates the RyR2 leading to increased SR Ca-sparks and DADs [35]. We therefore performed experiments using a CaMKII inhibitor and could show that AIP potently suppresses cellular triggers for arrhythmias as it was seen for Ran. Therefore, CaMKII seems to play an important role by mediating an I_{NaL} -induced leakiness of the cardiac RyR2 as demonstrated by a reduced Ca spark frequency in the presence of AIP. Ca-sparks and waves can give rise to DADs which in turn induce I_{TI} causing triggered activity. Our present study thus demonstrates that inhibition of I_{NaL} either by applying Ran or AIP exerts potent antiarrhythmic effects on the cellular level.

4.5 Molecular basis of altered I_{NaL} in heart failure

Na channels are multi-protein complexes and their activity is both determined by the pore-forming alpha subunit and additional interacting partners [8]. In our model overexpression of Nav1.5 could not explain the slowed I_{NaL} decay time five weeks after TAC (~57%), because Nav1.5. was already increased after one week (~192%) which interestingly had no significant effects on I_{NaL} .

In-vivo knockdown of the beta1-subunit accelerates the decay time of I_{Na} [20] and an increased expression might therefore augment the I_{NaL} . Because the expression was increased at both time points a sole upregulation of the beta1-subunit does not explain an increased I_{NaL} . Normalization of the beta1-subunit to the alpha-subunit expression (Nav1.5) shows a decrease after one week and normalization after 5 weeks of TAC and this might contribute to the observed I_{NaL} -changes, especially the relative downregulation after one week could have prevented an increase in I_{NaL} . Neuronal isoforms of Na channels have been described to be upregulated in a rat TAC model before [28]. In our study Nav1.1 was upregulated whereas Nav1.6 was downregulated after 5 weeks of TAC surgery. Thus, a contribution of Nav1.1 to the augmented I_{NaL} could be an underlying mechanism, but this correlation remains highly speculative.

CaMKII can induce I_{NaL} by phosphorylation of Nav1.5 [2, 36]. CaMKII activity measured by phosphorylation at Thr-286 was increased after TAC surgery. This increase was much higher at five vs. one week post-TAC. Conclusively, I_{NaL} decay time was only significantly slowed five weeks after TAC surgery. Recently, different phosphorylation sites of the cardiac Na channels were described [21, 22].

In our study the CaMKII-dependent phosphorylation site of the Nav1.5 at Ser571 was significantly more phosphorylated in the late compared to the early time point after TAC intervention (Figure 6A and G), consistent with previous findings of increased phosphorylation at Ser571 in non-ischemic human heart failure [36]. Taken together with our functional findings, CaMKII seems to prominently mediate the augmentation of I_{NaL} in the progression of pressure overload-induced heart disease.

Conversely, increased cellular Ca has been shown to activate CaMKII which in turn induces I_{NaL} by phosphorylation of Na channels [2, 37], which might thus constitute a vicious circle. This pathway has been demonstrated by Yao and coworkers who showed that a Nav1.5-dependent increase in Na influx leads to activation of CaMKII, which phosphorylates Nav1.5, further promoting Na influx [32]. However, it should be also mentioned that there is one report showing that Ran directly influences RyR2 open probability, desensitizes Ca-dependent RyR2 activation and inhibits Ca oscillations which needs to be further investigated [38]. On the other hand ATX-II induces spontaneous diastolic Ca release from the SR and DADs which would rather support the indirect effect of Ran on RyR2 open probability via modulation of I_{NaL} [39,40]. Most importantly DADs can be also abolished by application of TTX which probably supports an I_{NaL} -dependent effect on DAD induction [7].

Taken together, activation of CaMKII and CaMKII-dependent augmentation of I_{NaL} via Na channel phosphorylation seems to be a major mechanism underlying the increase in I_{NaL} , APD prolongation, and induction of cellular arrhythmogenic triggers observed five weeks post-TAC.

4.6 Limitations

The difference in phenotype between animals after one vs. five weeks of TAC is a decrease in heart function, but also a further increase in hypertrophy (heart weight). Both changes occur at the same time and therefore low degree compensated hypertrophy and high degree decompensated hypertrophy but with heart failure might be the best definition of the phenotypes. I_{NaL} seems to be the major contributor to the AP prolongation at low frequencies where I_{NaL} is prominent e.g. 0.5-2 Hz at least in our model. However, higher frequencies were not investigated in this work. Possibly, other channels and currents might be involved in the AP prolongation at higher frequencies. Finally, all experiments were performed on a single cell level, making a direct translation of our results and conclusions regarding arrhythmias into an in-vivo situation difficult (e.g. no electrical cell to cell conduction). Therefore, because of the absence of data to indicate that ranolazine impacts global arrhythmia susceptibility in this model, the investigation is limited to describing the potential mechanisms by which late I_{NaL} contributes to cellular arrhythmia susceptibility during heart failure.

4.7 Conclusions

The progression of pressure overload-induced heart failure is paralleled by changes of I_{NaL} and APD. In our model, hypertrophy with preserved systolic contractility was not associated with either an effect on I_{NaL} decay time or a prolongation of the APD. However, when hearts developed LV pump failure I_{NaL} increased along with AP prolongation. Inhibition of

I_{NaL} as well as CaMKII could largely counteract the AP prolongation in heart failure indicating a significant contribution of I_{NaL} and CaMKII (likely via I_{NaL}) on AP prolongation in the failing heart. A CaMKII-enhanced I_{NaL} appears to play a crucial role in the development of cellular arrhythmias associated with the progression of pressure overload-induced heart failure. Inhibition of I_{NaL} and CaMKII in order to suppress arrhythmias in heart failure merits further investigation.

Supplementary Material

Refer to Web version on PubMed Central for supplementary material.

Acknowledgments

We gratefully acknowledge the expert assistance of T. Schulte, S. Wollborn, and T. Sowa.

Funding This work was supported by grants from the Deutsche Forschungsgemeinschaft through SFB 1002 (K.T., G.H., L.S.M., S.S.), Heisenberg program Ma1982/4-2 (L.S.M.), and GRK 1816 RP3 (L.S.M., S.W.), Deutsches Zentrum für Herz-Kreislauf-Forschung (L.S.M., G.H.), Fondation Leducq (L.S.M., P.J.M.), Deutsche Gesellschaft für Kardiologie (C.M.S.), German Heart Foundation/German Foundation of Heart Research, Research Program, Faculty of Medicine of the University (S.S.), Saving Tiny Hearts Society, NIH (P.J.M.: HL084583, HL083422; T.J.H.: HL096805, HL114893), and AHA Established Investigator Award (P.J.M.).

References

- [1]. Bers, DM. Excitation-Contraction Coupling and Cardiac Contractile Force. 2nd ed. Kluwer Academic Publishers; Dordrecht, Netherlands: 2001.
- [2]. Wagner S, Dybkova N, Rasenack EC, Jacobshagen C, Fabritz L, Kirchhof P, et al. Ca^{2+} /calmodulin-dependent protein kinase II regulates cardiac Na^+ channels. *J Clin Invest.* 2006; 116:3127–38. [PubMed: 17124532]
- [3]. Undrovinas NA, Maltsev VA, Belardinelli L, Sabbah HN, Undrovinas A. Late sodium current contributes to diastolic cell Ca^{2+} accumulation in chronic heart failure. *J Physiol Sci.* 2010; 60:245–57. [PubMed: 20490740]
- [4]. Undrovinas AI, Maltsev VA, Sabbah HN. Repolarization abnormalities in cardiomyocytes of dogs with chronic heart failure: role of sustained inward current. *Cell Mol Life Sci.* 1999; 55:494–505. [PubMed: 10228563]
- [5]. Sossalla S, Maurer U, Schotola H, Hartmann N, Didié M, Zimmermann W, et al. Diastolic dysfunction and arrhythmias caused by overexpression of CaMKII δ C can be reversed by inhibition of late Na^+ current. *Basic Res Cardiol.* 2011; 106:263–72. [PubMed: 21174213]
- [6]. Song Y, Shryock JC, Wagner S, Maier LS, Belardinelli L. Blocking late sodium current reduces hydrogen peroxide-induced arrhythmogenic activity and contractile dysfunction. *J Pharmacol Exp Ther.* 2006; 318:214–22. [PubMed: 16565163]
- [7]. Song Y, Shryock JC, Belardinelli L. An increase of late sodium current induces delayed afterdepolarizations and sustained triggered activity in atrial myocytes. *Am J Physiol Heart Circ Physiol.* 2008; 294:H2031–9. [PubMed: 18310511]
- [8]. Maltsev VA, Undrovinas A. Late sodium current in failing heart: friend or foe? *Prog Biophys Mol Biol.* 2008; 96:421–51. [PubMed: 17854868]
- [9]. Maltsev VA, Sabbah HN, Higgins RS, Silverman N, Lesch M, Undrovinas AI. Novel, ultraslow inactivating sodium current in human ventricular cardiomyocytes. *Circulation.* 1998; 98:2545–52. [PubMed: 9843461]
- [10]. Belardinelli L, Shryock JC, Fraser H. Inhibition of the late sodium current as a potential cardioprotective principle: effects of the late sodium current inhibitor ranolazine. *Heart.* 2006; 92 Suppl 4:iv6–iv14. [PubMed: 16775092]
- [11]. Despa S, Islam MA, Weber CR, Pogwizd SM, Bers DM. Intracellular Na^+ concentration is elevated in heart failure but Na^+/K^+ pump function is unchanged. *Circulation.* 2002; 105:2543–8. [PubMed: 12034663]

- [12]. Valdivia CR, Chu WW, Pu J, Foell JD, Haworth RA, Wolff MR, et al. Increased late sodium current in myocytes from a canine heart failure model and from failing human heart. *J Mol Cellular Cardiol.* 2005; 38:475–83. [PubMed: 15733907]
- [13]. Ju YK, Saint DA, Gage PW. Hypoxia increases persistent sodium current in rat ventricular myocytes. *J Physiol.* 1996; 497:337–47. [PubMed: 8961179]
- [14]. Sossalla S, Maier LS. Role of ranolazine in angina, heart failure, arrhythmias, and diabetes. *Pharmacology and Therapeutics.* 2012; 133:311–22. [PubMed: 22133843]
- [15]. Maltsev VA, Silverman N, Sabbah HN, Undrovinas AI. Chronic heart failure slows late sodium current in human and canine ventricular myocytes: implications for repolarization variability. *Eur J Heart Fail.* 2007; 9:219–27. [PubMed: 17067855]
- [16]. Sossalla S, Fluschnik N, Schotola H, Ort KR, Neef S, Schulte T, et al. Inhibition of elevated Ca^{2+} /calmodulin-dependent protein kinase II improves contractility in human failing myocardium. *Circ Res.* 2010; 107:1150–61. [PubMed: 20814023]
- [17]. Lederer WJ, Tsien RW. Transient inward current underlying arrhythmogenic effects of cardiotoxic steroids in Purkinje fibres. *J Physiol.* 1976; 263:73–100. [PubMed: 1018270]
- [18]. Sossalla S, Wagner S, Rasenack EC, Ruff H, Weber SL, Schondube FA, et al. Ranolazine improves diastolic dysfunction in isolated myocardium from failing human hearts-role of late sodium current and intracellular ion accumulation. *J Mol Cellular Cardiol.* 2008; 45:32–43. [PubMed: 18439620]
- [19]. Sossalla S, Kallmeyer B, Wagner S, Mazur M, Maurer U, Toischer K, et al. Altered Na^{+} currents in atrial fibrillation effects of ranolazine on arrhythmias and contractility in human atrial myocardium. *J Am Coll Cardiol.* 2010; 55:2330–42. [PubMed: 20488304]
- [20]. Mishra S, Undrovinas NA, Maltsev VA, Reznikov V, Sabbah HN, Undrovinas A. Post-transcriptional silencing of SCN1B and SCN2B genes modulates late sodium current in cardiac myocytes from normal dogs and dogs with chronic heart failure. *Am J Physiol Heart Circ Physiol.* 2011; 301:H1596–605. [PubMed: 21705762]
- [21]. Hund TJ, Koval OM, Li J, Wright PJ, Qian L, Snyder JS, et al. A beta(IV)- spectrin/CaMKII signaling complex is essential for membrane excitability in mice. *J Clin Invest.* 2010; 120:3508–19. [PubMed: 20877009]
- [22]. Ashpole NM, Herren AW, Ginsburg KS, Brogan JD, Johnson DE, Cummins TR, et al. Ca^{2+} /calmodulin-dependent protein kinase II (CaMKII) regulates cardiac sodium channel $NaV1.5$ gating by multiple phosphorylation sites. *J Biol Chem.* 2012; 287:19856–69. [PubMed: 22514276]
- [23]. Boulaksil M, Winckels SK, Engelen MA, Stein M, van Veen TA, Jansen JA, et al. Heterogeneous Connexin43 distribution in heart failure is associated with dispersed conduction and enhanced susceptibility to ventricular arrhythmias. *Eur J Heart Fail.* 2010; 12:913–21. [PubMed: 20534605]
- [24]. Toischer K, Rokita AG, Unsold B, Zhu W, Kararigas G, Sossalla S, et al. Differential cardiac remodeling in preload versus afterload. *Circulation.* 2010; 122:993–1003. [PubMed: 20733099]
- [25]. Antzelevitch C, Belardinelli L, Zygmunt AC, Burashnikov A, DiDiego JM, Fish JM, et al. Electrophysiological effects of ranolazine, a novel antianginal agent with antiarrhythmic properties. *Circulation.* 2004; 110:904–10. [PubMed: 15302796]
- [26]. Maltsev VA, Undrovinas AI. Relationship between steady-state activation and availability of cardiac sodium channel: evidence of uncoupling. *Cell Mol Life Sci.* 1998; 54:148–51. [PubMed: 9539956]
- [27]. Undrovinas AI, Belardinelli L, Undrovinas NA, Sabbah HN. Ranolazine improves abnormal repolarization and contraction in left ventricular myocytes of dogs with heart failure by inhibiting late sodium current. *J Cardiovasc Electrophysiol.* 2006; 17(Suppl 1):S169–S77. [PubMed: 16686675]
- [28]. Xi Y, Wu G, Yang L, Han K, Du Y, Wang T, et al. Increased late sodium currents are related to transcription of neuronal isoforms in a pressure-overload model. *Eur J Heart Fail.* 2009; 11:749–57. [PubMed: 19584134]

- [29]. Wu L, Shryock JC, Song Y, Belardinelli L. An increase in late sodium current potentiates the proarrhythmic activities of low-risk QT-prolonging drugs in female rabbit hearts. *J Pharmacol Exp Ther.* 2006; 316:718–26. [PubMed: 16234410]
- [30]. Wu L, Rajamani S, Shryock JC, Li H, Ruskin J, Antzelevitch C, et al. Augmentation of late sodium current unmasks the proarrhythmic effects of amiodarone. *Cardiovasc Res.* 2008; 77:481–8. [PubMed: 18006430]
- [31]. Aiba T, Hesketh GG, Liu T, Carlisle R, Villa-Abrille MC, O'Rourke B, et al. Na⁺ channel regulation by Ca²⁺/calmodulin and Ca²⁺/calmodulin-dependent protein kinase II in guinea-pig ventricular myocytes. *Cardiovasc Res.* 2010; 85:454–63. [PubMed: 19797425]
- [32]. Yao L, Fan P, Jiang Z, Viatchenko-Karpinski S, Wu Y, Kornyejev D, et al. Nav1.5- dependent persistent Na⁺ influx activates CaMKII in rat ventricular myocytes and N1325S mice. *Am J Physiol Cell Physiol.* 2011; 301:C577–86. [PubMed: 21677263]
- [33]. Klensch H. The basal noradrenaline level in human peripheral venous blood. *Pflugers Arch Gesamte Physiol Menschen Tiere.* 1966; 290:218–24.
- [34]. Pieske B, Maier LS, Piacentino V 3rd, Weisser J, Hasenfuss G, Houser S. Rate dependence of [Na⁺]_i and contractility in nonfailing and failing human myocardium. *Circulation.* 2002; 106:447–53. [PubMed: 12135944]
- [35]. Mallwitz A, Sag CM, Sossalla ST, Hartmann N, Steuer N, Sowa T, et al. CaMKII-dependent SR Ca leak contributes to proarrhythmogenic effects of increased late Na current in isolated cardiac myocytes. *Clin Res Cardiol.* 2011; (Suppl 1)
- [36]. Koval OM, Snyder JS, Wolf RM, Pavlovicz RE, Glynn P, Curran J, et al. Ca²⁺/calmodulin-dependent protein kinase II-based regulation of voltage-gated Na⁺ channel in cardiac disease. *Circulation.* 2012; 126:2084–94. [PubMed: 23008441]
- [37]. Ma J, Luo A, Wu L, Wan W, Zhang P, Ren Z, et al. Calmodulin kinase II and protein kinase C mediate the effect of increased intracellular calcium to augment late sodium current in rabbit ventricular myocytes. *Am J Physiol Cell Physiol.* 2011; 15:C1141–51. [PubMed: 22189558]
- [38]. Parikh A, Mantravadi R, Kozhevnikov D, Roche MA, Ye Y, Owen LJ, et al. Ranolazine stabilizes cardiac ryanodine receptors: a novel mechanism for the suppression of early afterdepolarization and torsades de pointes in long QT type 2. *Heart Rhythm.* 2012; 9:953–60. [PubMed: 22245792]
- [39]. Wasserstrom JA, Sharma R, O'Toole MJ, Zheng J, Kelly JE, Shryock J, et al. Ranolazine antagonizes the effects of increased late sodium current on intracellular calcium cycling in rat isolated intact heart. *J Pharmacol Exp Ther.* 2009; 331:382–91. [PubMed: 19675298]
- [40]. Song Y, Shryock JC, Wu L, Belardinelli L. Antagonism by ranolazine of the pro-arrhythmic effects of increasing late I_{Na} in guinea pig ventricular myocytes. *J Cardiovasc Pharmacol.* 2004; 44:192–9. [PubMed: 15243300]

Highlights

- I_{NaL} is enhanced in heart failure but not in compensated hypertrophy
- Increased I_{NaL} causes action potential prolongation in heart failure
- These changes trigger cellular arrhythmias which are prevented by I_{NaL} and CaMKII inhibition
- CaMKII regulates I_{NaL} and thereby cellular arrhythmias via phosphorylation of the $Na_v1.5$

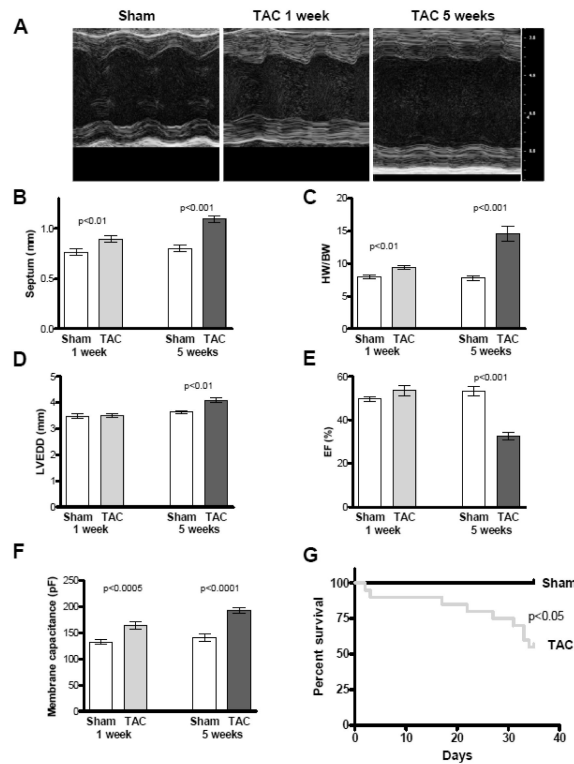


Figure 1. Echocardiographic data

Cardiac phenotype characteristics. **A** Representative echocardiographic recordings of sham and TAC mice 1 and 5 weeks after intervention (1 week: sham n=6, TAC n=10, 5 weeks: sham n=10, TAC n=15). **B** Mean values of septum width. **C** Mean values of heart weight / body weight ratio (HW/BW). **D** Mean values of ejection fraction (EF). **E** Mean values of left ventricular end-diastolic diameter (LVEDD). **F** Mean values of membrane capacitances. **G** Kaplan-Meier survival curve of sham and TAC animals which does not include mortality within the first 24 hrs post-TAC surgery.

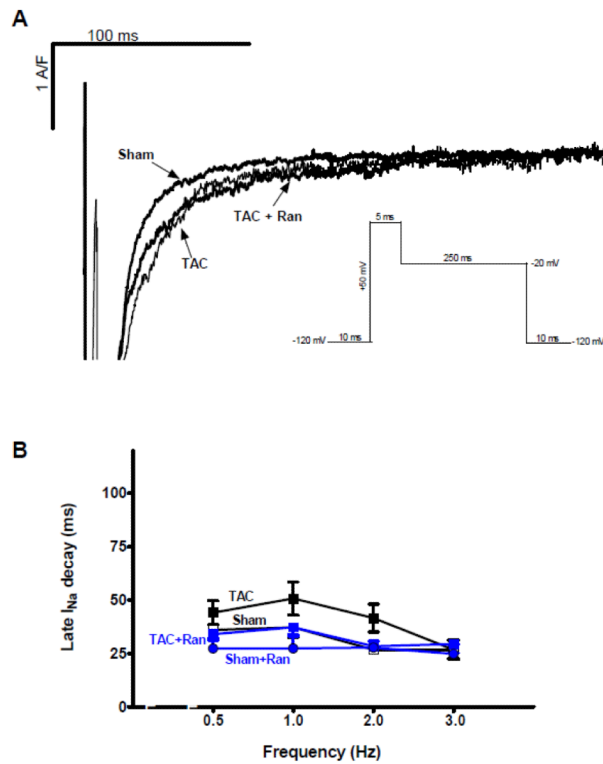


Figure 2. Effects of TAC on late I_{Na} after one week

Measurements of I_{NaL} after one week of pressure overload. **A** Original recordings showing I_{NaL} in sham and TAC cells paced at 0.5 Hz in the presence of vehicle or ranolazine. **B** Mean values of I_{NaL} decay time in the corresponding groups (TAC 20, sham 14, TAC+Ran 7, sham+Ran 6 cells, no statistical differences between the groups using 2-way RM ANOVA).

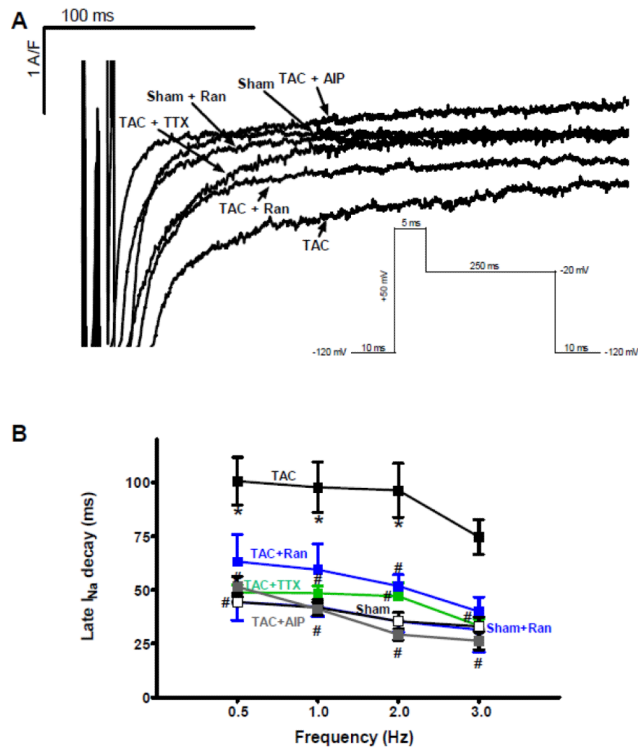


Figure 3. Effects of TAC on late I_{Na} after 5 weeks

Measurements of I_{NaL} after five weeks of TAC surgery. **A** Original tracings showing recorded I_{NaL} in sham and TAC cells in the presence of either vehicle, Ran, TTX, and AIP (in TAC) paced at 0.5 Hz. **B** Mean values of I_{NaL} decay time in the corresponding groups. There was a statistical difference between I_{NaL} decay time of TAC vs. sham ($n=26$ vs.7), TAC vs. TAC+Ran ($n=17$), TAC vs. TAC+TTX ($n=16$), TAC vs. TAC+AIP ($n=18$) vs. TAC. $*=p < 0.05$ vs. sham $\#=p < 0.05$ vs. TAC

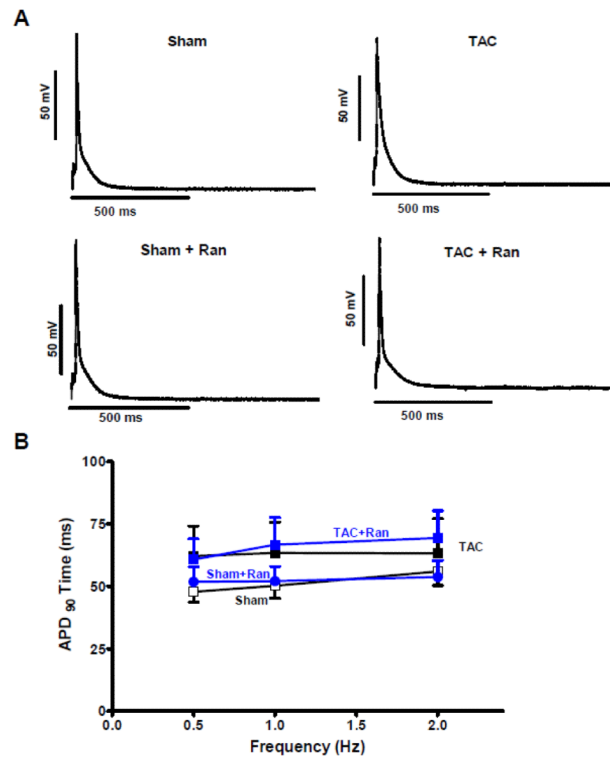


Figure 4. Effects of TAC on action potentials after 1 week

Measurements of APs after one week of TAC intervention. **A** Original tracings showing recorded APs in sham and TAC cells in the presence of vehicle or Ran paced at 0.5 Hz. **B** Mean values of APD (90%) in the corresponding groups (TAC 7, sham 12, TAC+Ran 19, sham+Ran 15 cells, no statistical differences between the groups using 2-way RM ANOVA).

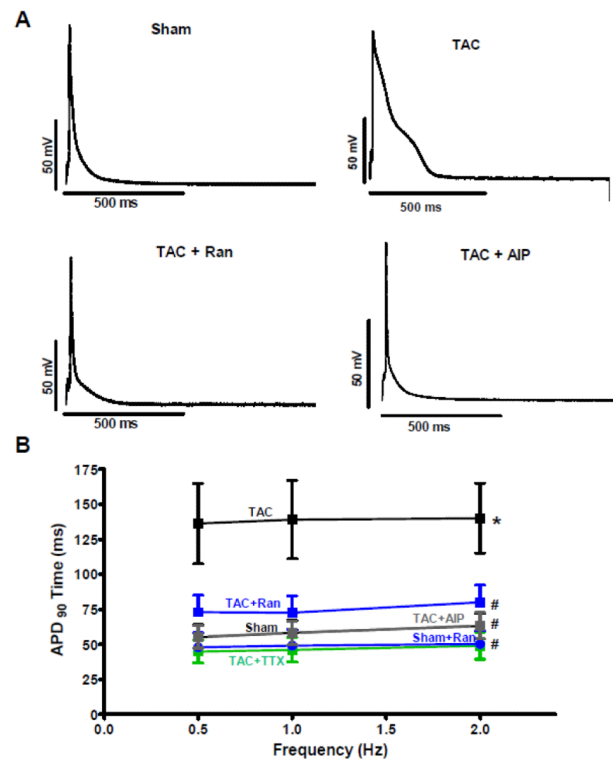


Figure 5. Effects of TAC on action potentials after 5 week

Measurements of APs in cells isolated from animals five weeks after TAC surgery. **A** Original tracings showing recorded action potentials in sham and TAC cells in the presence of vehicle, Ran, and AIP paced at 0.5 Hz. **B** Mean values of (APD₉₀) in the corresponding groups. (TAC 15, sham 8, TAC+Ran 19, TAC+AIP 18, TAC+TTX 10 cells. *=p<0.05 vs. sham #=p<0.05 vs. TAC

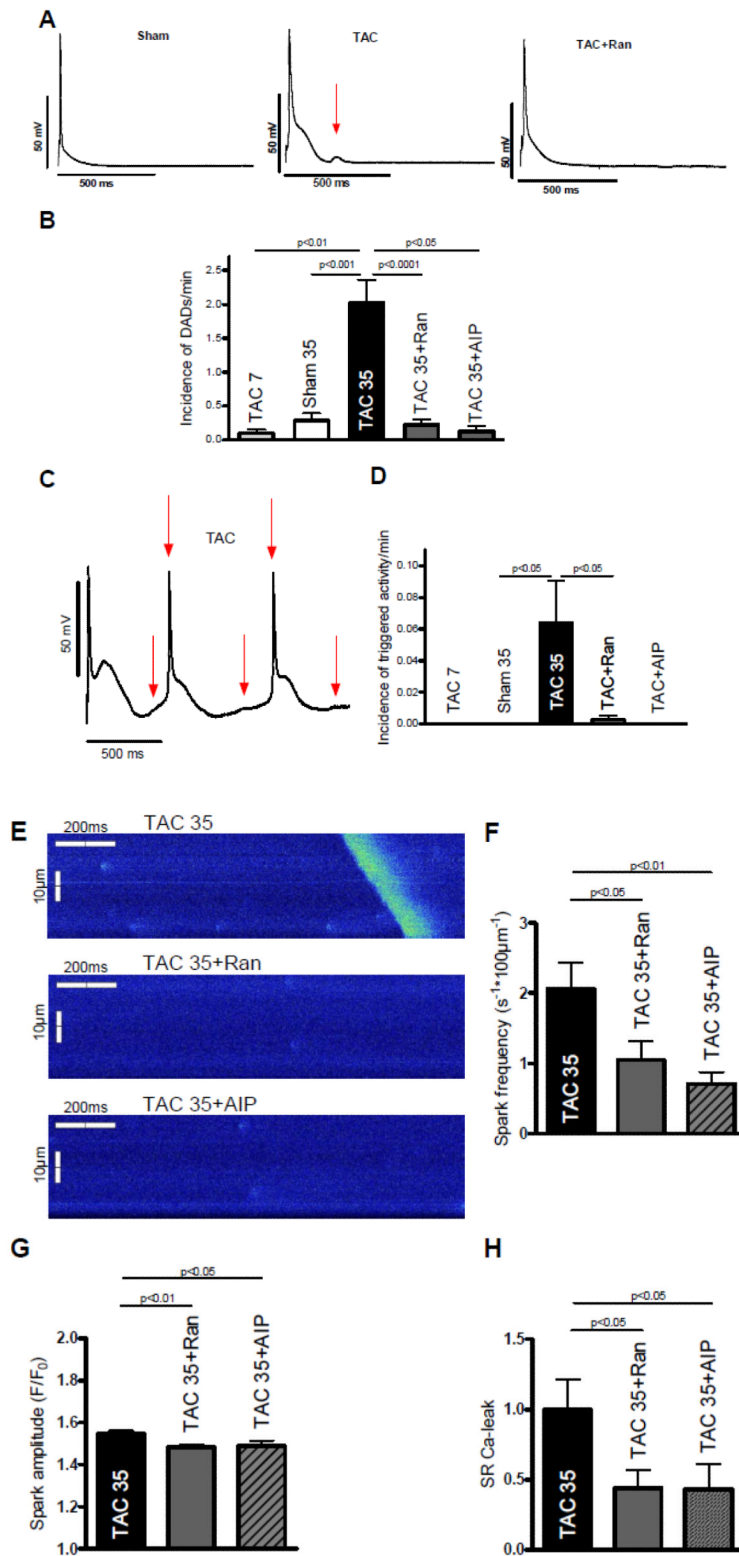


Figure 6. Arrhythmic triggers and SR Ca-leak

Measurements of APs five weeks after TAC surgery in the presence of 10^{-8} mol/L isoproterenol. **A** Original tracing of APs in the presence of isoproterenol. Red arrows indicate DADs. **B** Mean values of DAD-incidence in sham (n=15), TAC (n=20), Ran-treated (n=15) and AIP-treated TAC cells (n=5). **C** Original tracing of spontaneous APs in the presence of isoproterenol. Red arrows indicate triggered activity (unstimulated APs). **D** Mean values of triggered activity (meaning unstimulated APs). **E** Representative confocal line scans of cardiomyocytes under control conditions (above) as well as upon ranolazine (middle) and AIP-treatment (below) showing Ca-sparks and a diastolic Ca-wave (in control group). **F** Inhibition of I_{NaL} by ranolazine as well as CaMKII inhibition by AIP significantly decrease the frequency of diastolic Ca-sparks (n=30-38). **G** The amplitude of diastolic Ca-sparks is significantly reduced in the presence of ranolazine (n=80 vs. 128, control) as well as after CaMKII-inhibition with AIP (n=41). **H** The inhibitors yield a significant decrease of the resulting calculated SR Ca-leak (CaSpF – amplitude – duration – width, normalized to control group).

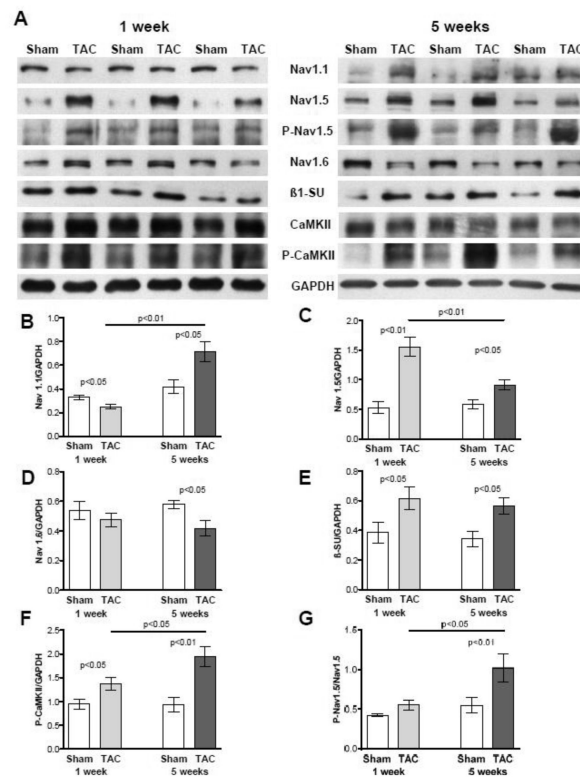


Figure 7. Protein analysis of CaMKII δ and Na channel isoforms (n=6 per group and time point). **A** Exemplary western blots. **B** Mean values of Na channel isoform α 1.1 normalised to GAPDH. **C** Mean values of Na channel isoform α 1.5 normalised to GAPDH. **D** Mean values of Na channel isoform α 1.6 normalised to GAPDH. **E** Mean values of beta1 subunit normalised to GAPDH. **F** Mean values of phosphorylated CaMKII δ (at Thr-287) normalised to GAPDH. **G** Mean values of phosphorylated Nav1.5 at Ser571 (CaMKII phosphorylation site) normalised to total Nav1.5.